Electronic and magnetic properties of Cm in $Pb_2Sr_2Cm_{1-x}Ca_xCu_3O_8$ ($x=0.0$ and 0.5)

S. Skanthakumar, C. W. Williams, and L. Soderholm
Chemistry Division, Argonne National Laboratory, Argonne, Illinois 60439
(Received 10 May 2001; published 24 September 2001)

A combination of x-ray diffraction, x-ray absorption spectroscopy, and magnetic susceptibility measurements have been used to study the physical properties of $Pb_2Sr_2Cm_{1-x}Ca_xCu_3O_8$ ($x=0.0,0.5$). These Cm compounds are isostructural with the superconducting members of the $Pb_2Sr_2R_{1-x}Ca_xCu_3O_8$ (R denotes rare earth) series. X-ray absorption and magnetic susceptibility data clearly indicate that the Cm is trivalent in this compound, consistent with the superconducting members of this series. However, $Pb_2Sr_2Cm_{0.5}Ca_{0.5}Cu_3O_8$ is not superconducting. Furthermore, the Cm spins are found to magnetically order in the parent compound $Pb_2Sr_2CmCu_3O_8$ with an ordering temperature of 18 K. Suppression of superconductivity is observed together with high-magnetic ordering temperatures in other high-T_c related compounds synthesized with Cm. The results determined here are put into context with these previous observations.

DOI: 10.1103/PhysRevB.64.144521 PACS number(s): 74.72.−h, 75.30.Et, 61.10.Ht

I. INTRODUCTION

The rare-earth (R) substitution effects on the high-T_c series $RBa_2Cu_3O_7$, $R_{2-x}Ce_xCuO_4$, and $Pb_2Sr_2R_{1-x}Ca_xCu_3O_8$ have been studied in great detail using a wide variety of experimental techniques.[1] The superconducting behavior exhibited by these three different series of substituted Cu oxides are generally not affected by the nature of R, although the R may carry magnetic moments as high as $10\mu_B$. Magnetic quenching of superconductivity does not occur in these materials because the superconducting electrons reside in the planar CuO bands and the CuO and R sublattices are effectively electronically decoupled. This isolation is consistent with the known electronic behavior of the $4f$ electrons, which are generally well localized, and are well modeled by simple, single-ion approaches. Despite this general trend, there are several f ions that, when substituted into one or more of the series listed above, do have a pronounced effect on superconductivity. These ions, which include Ce, Pr, Tb, Am ($Z=95$) and Cm ($Z=96$), can be divided into two classes. The R ion in the Ce and Am analogs, if formed, are tetravalent,[2,3] whereas all the other R are trivalent. It has been demonstrated that the introduction of a tetravalent R suppresses superconductivity. The extra charge introduced by the Ce^{4+} or Am^{4+} is transferred to the CuO_2 planes, reducing the charge carriers. The situation is different with the R for Pr and Cm analogs of these materials. Both these ions appear to be trivalent and yet Cm, and sometimes Pr, suppress superconductivity through a mechanism that is not yet completely understood.[4] However, it is clear that when T_c is suppressed the R moments order at anomalously high temperatures.

The parent compounds $Pb_2Sr_2R_{1-x}Ca_xCu_3O_8$, for which $x=0$, form an isostructural series over a wide range of R, including Y, La-Lu (Refs. 5 and 6) and the actinide Am.[3] The parent compounds themselves are not superconducting, although superconductivity can be induced by oxidizing some Cu^{2+}, either by making the sample substoichiometric in R^{3+}, or by replacing some R^{3+} with Ca^{2+}.[7] Generally superconductivity is observed for $0.2<x<0.8$ in $Pb_2Sr_2R_{1-x}Ca_xCu_3O_8$, with the optimum Ca concentration of 0.5 for highest T_c. The superconducting critical temperatures T_c are about 70 K for most of the series, although T_c is 61 K for the Pr analog, about 10 K lower than the rest of the series. Magnetic and inelastic neutron scattering studies have shown Pr to be essentially trivalent in $Pb_2Sr_2PrCu_3O_8$.[8] It should be noted that the Pr moments order at 6 K,[9,10] which is significantly higher than the other R substitutes, despite the relatively small local moment on Pr. In contrast to the other members of the series, neither the Ce nor the Am analog has been found to be superconducting. Detailed studies of these analogs have shown that, although the compounds are isostructural with other members of this series, both Ce and Am are tetravalent.[2,3] In the work presented here, we have synthesized the R for Cm member of the $Pb_2Sr_2R_{1-x}Ca_xCu_3O_8$ series for $x=0$ and 0.5, and have characterized their structural and magnetic properties. X-ray absorption near-edge structure (XANES) experiments were conducted near the Cm L_3, L_2, and L_1 edges in order to ascertain the oxidation state of Cm. XANES has been used extensively to determine the ion-specific valence states in complex compounds.[11] The atomic structure was determined by combining x-ray powder diffraction and extended x-ray-absorption fine structure (EXAFS) data. Cm has been chosen for this study because it has a tetravalent/trivalent reduction potential similar to Pr and Tb but its $5f$ orbitals have a slightly larger radial extent than the $4f$ orbitals of Pr. In addition, Cm^{3+} has a $S_{7/2}$ Russell-Saunders ground state that, to first order, is not influenced by the symmetry of the crystal field potential in which it is situated. These unique attributes form a contrast to the properties of the other members of the series and are expected to add insight into the suppression of superconductivity and the concomitant high magnetic ordering temperatures seen for Pr and Cm in other high-T_c related materials. Indeed, $Pb_2Sr_2Cm_{1-x}Ca_xCu_3O_8$ is not superconducting and the parent, $x=0$, compound exhibits evidence of magnetic ordering of the Cm moments at about 18 K.

II. EXPERIMENTAL DETAILS

Powder samples of $Pb_2Sr_2Cm_{1-x}Ca_xCu_3O_8$ ($x=0.0,0.5$) were prepared by solid-state reaction techniques. Since

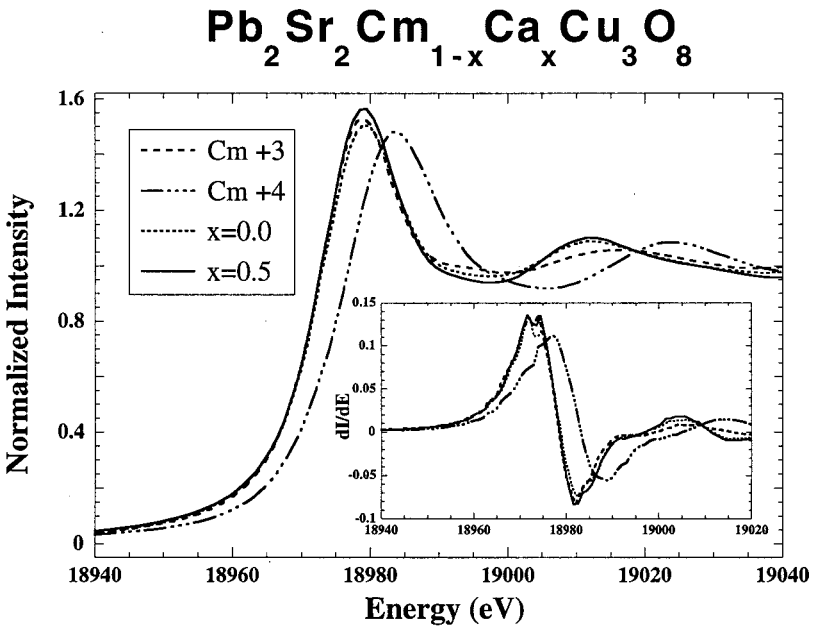

FIG. 1. The Cm L_3-edge XANES spectra for $Pb_2Sr_2Cm_{1-x}Ca_xCu_3O_8$ (x=0.0,0.5) with spectra of trivalent (Cm_2CuO_4) and tetravalent (CmO_2) standards. The fluorescence data are shown for $Pb_2Sr_2Cm_{1-x}Ca_xCu_3O_8$, while transmission data are shown for the standards. The inset shows the first derivative of the intensities. The similarity between the spectra obtained from Cm trivalent standard and $Pb_2Sr_2Cm_{1-x}Ca_xCu_3O_8$ indicates that Cm is trivalent in $Pb_2Sr_2Cm_{1-x}Ca_xCu_3O_8$.

^{248}Cm is a man-made radioactive isotope with limited availability, sample sizes were restricted to less than 10 mg. Details of the synthetic procedure were determined from surrogate work on the Pr analog because of the similarities of Pr and Cm solid-state chemistry. Stoichiometric ratios of PbO, CuO, $CaCO_3$, $SrCO_3$ and Cm as the oxalate, were mixed, pelletized, and prefired at 750 °C for two days in N_2 containing 2% O_2. The samples were reground, repelletized, and sintered at 750 °C under a N_2 atmosphere for two days. This procedure was repeated until the x-ray diffraction data, which were taken on a Scintag theta-theta diffractometer (Cu K_α radiation), showed the sample to be single phase. Room temperature x-ray diffraction data were analyzed using the general structure analysis system (GSAS) program.[12] Two wavelengths, $K_{\alpha 1}$ (1.5405 Å) and $K_{\alpha 2}$ (1.5443 Å), were used with a relative ratio of 0.5 for the structural refinement.

The magnetization experiments were conducted using a superconducting quantum interference device (SQUID) magnetometer over the temperature range of 5–320 K. Sample masses for $x=0.0$ and 0.5 were 3.23 and 6.98 mg, respectively. Magnetizations versus applied field were measured at 5 K to check the assumed linearity. A magnetic field of 500 G was used for susceptibility measurements whereas low magnetic fields (<20 G) were employed to detect superconductivity. Samples were doubly encapsulated in Al containers for these measurements to prevent radioactive contamination, and containers were run separately in order to correct the magnetization data for background. X-ray absorption experiments were conducted on powder samples at room temperature on the BESSRC bending magnet beam lines 12-BM-B at the Advanced Photon Source (APS) at the Argonne National Laboratory. Cm-L_1, L_2, and L_3 edge data were collected employing a Si(111) double-crystal monochromator that gives an energy resolution of $\Delta E/E=14.1\times10^{-5}$. The high critical energy of the APS ring required the use of a Pt mirror to remove the higher-order harmonics. Nb foil was used to calibrate the energy at 18 986 eV. CmO_2 and Cm_2CuO_4 are used as the tetravalent and trivalent Cm standards, respectively, and the other details of the x-ray absorption setup are described elsewhere.[13] Data were collected in the transmission and fluorescence modes simultaneously. $\mathrm{Ln}(I_o/I_t)$ and I_1/I_0 were used for normalization of transmitted and fluorescence intensities, respectively. Data analysis methodology is described elsewhere.[14] WINXAS data analysis software[15] was used to fit the EXAFS data. FEFF7.023 (Ref. 16) was used to obtain the phase and amplitude functions required for EXAFS refinement.

III. RESULTS

A. XANES

The Cm L_3 edge XANES spectra obtained from $Pb_2Sr_2Cm_{1-x}Ca_xCu_3O_8$, along with those of the trivalent (Cm_2CuO_4) and tetravalent (CmO_2) standards, are shown in Fig. 1.[13] The first derivative of the normalized intensities, used to determine the edge positions, are shown in the inset. The fingerprint of Cm^{3+} spectrum is the absorption energy (first peak of the derivative) at about 18 973 with the maximum absorption at 18 979 eV, whereas the absorption energy peak of Cm^{4+} is at 18 977 eV with maximum absorption at 18 984 eV. The observed 4 eV shifts between trivalent and tetravalent Cm absorption edges is consistent with the magnitude in differences observed between other trivalent and tetravalent actinides.[3,17–19] XANES data for both the $x=0.0$ and 0.5 compounds of $Pb_2Sr_2Cm_{1-x}Ca_xCu_3O_8$ are indistinguishable from those of the trivalent Cm standard. Our measurements of L_2 and L_1 edges also showed similar shifts in energy between trivalent and tetravalent Cm. L_2 and L_1 edges are observed to be at 23 262 and 24 547 eV for trivalent Cm_2CuO_4 and $Pb_2Sr_2Cm_{1-x}Ca_xCu_3O_8$, whereas they are at 23 266 and 24 551 eV for the tetravalent CmO_2. These observations show that Cm is essentially trivalent in

TABLE I. Structural parameters for $Pb_2Sr_2Cm_{1-x}Ca_xCu_3O_8$ ($x=0.0$ and 0.5) obtained from refinement of the x-ray diffraction and x-ray absorption fine structure (XAFS) data taken at room temperature. In *Cmmm* (No. 65), the crystallographic sites for Cm/Ca, Pb, Sr, Cu1, Cu2, O1, O2, O3 are $2a$, $4l$, $4k$, $2d$, $4l$, $4l$, $8m$, and $16r$, and their coordinates are (0, 0, 0) (0, $\frac{1}{2}$, z), (0, 0, z), (0, 0, $\frac{1}{2}$), (0,$\frac{1}{2}$, z), (0, $\frac{1}{2}$, z), ($\frac{1}{4}$, $\frac{1}{4}$, z), and (x, y, z), respectively. The occupation factor for O3 is 0.25. Coordinates of Pb, Sr, and Cu2 are obtained using diffraction data while O2 coordinates were fixed to the value obtained from absorption data. O1 and O3 were fixed at (0, 0.5, 0.254) and (0.945, 0.072, 0.386).

	$x=0.0$	$x=0.5$
a (Å)	5.4378(1)	5.4253(1)
b (Å)	5.4756(1)	5.4605(1)
c (Å)	15.7902(4)	15.8055(4)
Volume (Å^3)	470.14(2)	468.23(2)
z for Pb	0.3885(2)	0.3904(2)
z for Sr	0.2253(3)	0.2241(3)
z for Cu2	0.1109(6)	0.1143(4)
	0.1108(35)[a]	0.1104(35)[a]
z for O2	0.093(3)[a]	0.094(3)[a]

[a]Parameters obtained from EXAFS fit.

$Pb_2Sr_2Cm_{1-x}CaCu_3O_8$ for both the $x=0$ and the Ca-doped sample. Ca doping does not measurably affect the Cm valence.

B. Crystal structure

In addition to the XANES, Cm-L_3 edge EXAFS data were also obtained. These data, in combination with x-ray powder diffraction data, have been used to determine that $Pb_2Sr_2Cm_{1-x}Ca_xCu_3O_8$ ($x=0,0.5$) are isostructural with the superconducting lanthanide analogs $Pb_2Sr_2R_{1-x}Ca_xCu_3O_8$. An x-ray Reitveld refinement, constrained to be consistent with the EXAFS results, was used to determine the lattice constants, space group, and overall structure. The EXAFS data were used to obtain the Cm-O and Cm-Cu distances, which are difficult to obtain from the x-ray diffraction data because of the very weak scattering from O and Cu atoms compared to the heavier atoms, such as Cm and Pb. Several iterations between fitting the EXAFS data and Reitveld refinements of the x-ray diffraction data were required before a consistent fit was obtained for all the data.

X-ray diffraction data, which were collected over the range of 5°–150° at room temperature, show the $Pb_2Sr_2Cm_{1-x}Ca_xCu_3O_8$ samples to be of high quality. All observed peaks can be indexed using the same orthorhombic space group *Cmmm* that was found for the other members of this series.[2] The absence of extra peaks in the diffraction pattern confirms the sample quality. Refined values for the lattice parameters determined from fitting these peak positions are given in Table I. The lattice parameters a and b are contracted whereas the c axis is elongated for the Ca-doped sample. Similar behavior was observed for other R analogs of $Pb_2Sr_2R_{1-x}Ca_xCu_3O_8$.[2,20] A comparison between unit-cell edges a,b and volume V for the Cm analog with the other

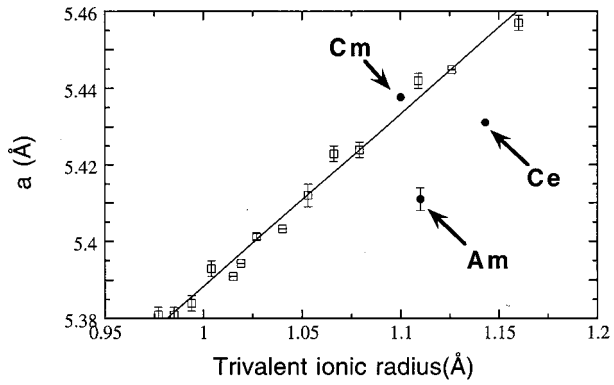

FIG. 2. Lattice parameter a of $Pb_2Sr_2RCu_3O_8$ as a function of trivalent (R^{3+}) ionic radius for various R. a for other R, and trivalent ionic radii were obtained elsewhere.[2,3,21,32] Line is drawn to show the trivalent trend. Cm is trivalent that whereas Am and Ce are tetravalent.

$Pb_2Sr_2RCu_3O_8$ compounds reveals good agreement of our data with the trend established for the trivalent R. The variation of the unit cell a axis as a function of trivalent ionic radii is shown in Fig. 2. The ionic radius of tetravalent Cm (0.95 Å) is significantly smaller than that of trivalent Cm (1.10 Å),[3,21] therefore the valence state of Cm is expected to influence significantly the lattice parameters. The lattice parameters a (Fig. 2) and b and unit-cell volume for various R in $Pb_2Sr_2RCu_3O_8$ increases smoothly with increasing trivalent ionic radii with the exception of R for Ce and Am. Ce and Am have been previously demonstrated to be tetravalent ions,[2,3] which have smaller ionic radii than that of their trivalent counterparts, therefore accounting for their deviation from the trend established by the trivalent ions. The lattice constants and volume for $Pb_2Sr_2CmCu_3O_8$ fall on the trend established by the trivalent ions, confirming our XANES results that showed Cm to be trivalent in this material.

Several space groups including tetragonal ($P4/mmm$),[22] orthorhombic (*Cmmm*, *Pman*, *Pmmm*),[23–26] and monoclinic ($C2/m$,$P2_1/m$,$P2_1$) (Refs. 27,28) have been reported for the $Pb_2Sr_2RCu_3O_8$ series. Although our data are consistent with, and are refined in, the space group *Cmmm*, a close inspection indicates that the (1, 1, 4) and (2, 0, 5) peaks are much broader than (0, 0, 2), (0, 2, 0), and (0, 2, 5) peaks. Similar behavior has been previously observed for other $Pb_2Sr_2R_{1-x}Ca_xCu_3O_8$, where it has been attributed to a slight monoclinic distortion with a distribution of the β angle.[2,29–31]

The x-ray diffraction data between 20° and 150°, together with the Cm L_3 EXAFS data, were used in the structural refinement. The diffraction data, over a selected energy range (Fig. 3), and the EXAFS data, together with their Fourier transform (Fig. 4), are shown for $Pb_2Sr_2Cm_{0.5}Ca_{0.5}Cu_3O_8$. The similarity between data from $Pb_2Sr_2Cm_{1-x}Ca_xCu_3O_8$ and those of the $4f$ compounds is demonstrated by the EXAFS data from $Pb_2Sr_2R_{1-x}Ca_xCu_3O_8$[3,32] that is also included in the EXAFS (Fig. 4) for R denoting Pr. Metrical results from the diffraction and EXAFS refinements are shown in Tables I and II, respectively.

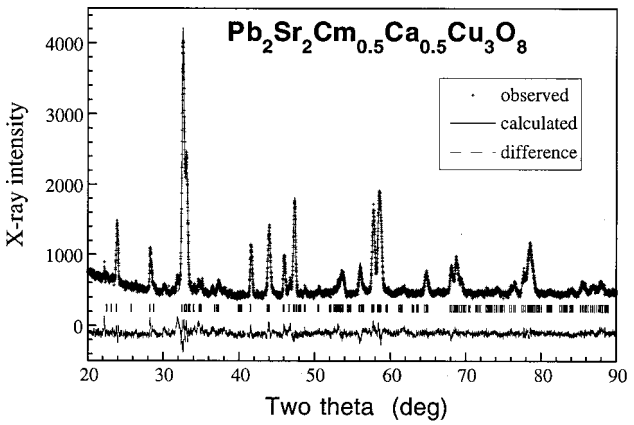

FIG. 3. X-ray diffraction pattern and refinement for $Pb_2Sr_2Cm_{0.5}Ca_{0.5}Cu_3O_8$ at room temperature. These data were collected with Cu K_α x-rays. The crosses are the observed data and the solid line is the refinement. The difference between the observed data and the refined structure is shown at the bottom. Vertical lines in the middle indicate the positions of symmetry allowed charge Bragg peaks originating from $K_{\alpha 1}$ and $K_{\alpha 2}$ x-rays.

The refinement was done in space group *Cmmm* (No. 65). The Cm/Ca and Cu1 positions are determined by symmetry. The *z* parameters for Pb and Sr were determined by Rietveld refinement of the diffraction data. The Cu2 position was determined both from the diffraction data and also from fitting the EXAFS Cm-Cu distance. The O2 position was determined directly from the EXAFS Cm-O fitting and held fixed in the diffraction refinement. The O1 and O3 positional parameters were estimated from previous structural work on the *R* analogs of this structure,[2,32] and were held fixed for the refinement. Their contribution is very small to the total x-ray scattering, which is dominated by the heavy atoms.

TABLE II. The parameters obtained by refining the room temperature Cm L_3 EXAFS data of $Pb_2Sr_2Cm_{1-x}Ca_xCu_3O_8$ ($x=0.0$ and 0.5). Coordination numbers were fixed at 8 for both O and Cu based on the space group.

		$x=0.0$	$x=0.5$
Cm-O	Cm-O (Å)	2.426(24)	2.436(24)
	σ^2 (Å^2)	0.022(3)	0.013(2)
	E_0 (eV)	−1.41	−0.69
Cm-Cu	Cm-Cu (Å)	3.241(30)	3.233(30)
	σ^2 (Å^2)	0.010(2)	0.007(2)
	E_0 (eV)	−1.41	−0.69

All coordination numbers for EXAFS fits were fixed using space group requirements. Introducing three or more fixed shells into the EXAFS fit to account for Cm-Sr, Cm-Cm, and Cm-O interactions with parameters determined either from the structural refinement or, in the case of Cm-O, from previous work on the Pr analog,[2,32] improves the fit. However, these new parameters that are introduced into the EXAFS model cannot be refined because there are insufficient data to support more than two shells fit. The refined Cm-O and Cm-Cu distances were 2.426(24) and 3.241(30)

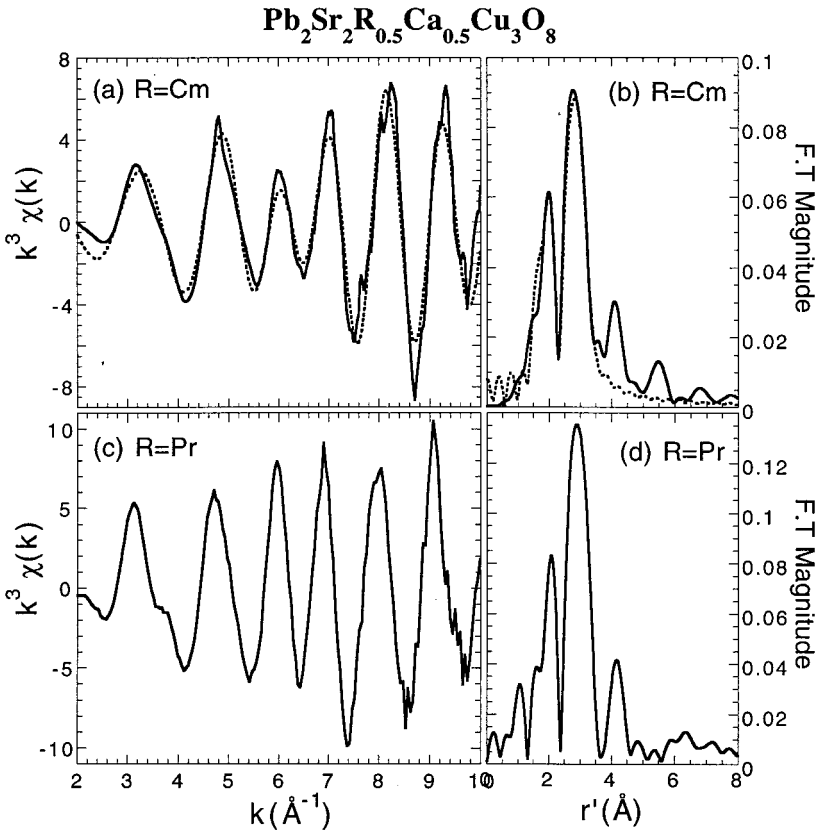

FIG. 4. (a) The Cm-L_3 edge fluorescence $k^3\chi(k)$ EXAFS data (solid line) from $Pb_2Sr_2Cm_{0.5}Ca_{0.5}Cu_3O_8$. The best fits using two Cm-O and Cm-Cu distances are shown as dashed lines. (b) Fourier transforms of the experimental (solid lines) and fitted (dashed lines) EXAFS data before phase shift correction. The Pr-L_3 edge EXAFS data and their Fourier transform for $Pb_2Sr_2Pr_{0.5}Ca_{0.5}Cu_3O_8$ are shown in (c) and (d), respectively.

Å, respectively, for the undoped sample ($x=0.0$) whereas they refined to 2.436(24) and 3.233(30) Å for the $x=0.5$ sample. It should be noted that the Cm-O-fitted Debye-Waller parameter for the parent compound is larger than expected relative to its doped counterpart. This result, reproducible and verified over different synchrotron runs, is unexpected and inconsistent with the higher degree of disorder normally associated with a doped material. It should be further noted that this result does not impact our Cm-O bond distance because it is the coordination number that is correlated with the Debye-Waller parameter. Our coordination numbers are fixed by space group considerations and not refined from the EXAFS data. The fits to the diffraction and EXAFS experimental data for $x=0.5$ compound are compared with the appropriate data in Figs. 3 and 4.

The Cm-O distances we obtained from the EXAFS are significantly larger than those of AmO and Ce-O in the same system.[3] This observation in consistent with Cm^{3+}, Am^{4+}, and Ce^{4+}, the latter two of which have smaller ionic radii than their trivalent counterparts. The effect of Ca doping on the Cm-O distance is also similar to that observed in other trivalent $4f$ compounds. When R is trivalent, R-O distances increase with Ca doping whereas they decrease in the tetravalent Ce analog.[2,33,34] Both x-ray diffraction and absorption experiments clearly indicate that $Pb_2Sr_2Cm_{1-x}Ca_xCu_3O_8$ is isostructural to all other $Pb_2Sr_2R_{1-x}Ca_xCu_3O_8$ compounds and Cm is trivalent in this system.

C. Magnetic susceptibility

Magnetic susceptibility data, obtained from a powder sample of $Pb_2Sr_2CmCu_3O_8$ and measured as a function of temperature, are shown in Fig. 5. The inverse susceptibility, shown in the inset, increases linearly with temperature above 30 K. These data were least squares fitted to the Curie-Weiss law $\chi=C/(T+\Theta)$, where C and Θ are Curie and Weiss constants. The refined parameters are $C=9.40$ K and $\Theta=96.8$ K for the data between 120 and 320 K. The effective moment of $8.7(2)\mu_B$, obtained from the measured C using $\mu_{\text{eff}}=(8C)^{1/2}$, is significantly larger than the $7.94\mu_B$ expected for a Cm^{3+} free-ion moment. Cm^{3+} has a spherically symmetric, $^8S_{7/2}$ ground state and therefore the crystal field will not influence the magnetic susceptibility to first order.[13] For comparison, tetravalent Cm has a $^7F_0$, $J=0$ Russell-Saunders ground state, and hence a free-ion moment of $0\mu_B$. Therefore, the high value of the effective moment observed here for $Pb_2Sr_2CmCu_3O_8$ can be accounted for neither by crystal-field effects nor by the presence of some tetravalent Cm. Instead, the large observed moment is evidence of a local paramagnetic moment on Cu. When the inverse magnetic susceptibility data fitted between 30 and 90 K, which is below the slight anomaly observed at about 100 K, an effective magnetic moment of $7.8(2)\mu_B$ is obtained in agreement with that expected for a Cm^{3+} free-ion moment. This result may indicate that Cu moment ordering occurs below 100 K. Precedent for a Cu local moment comes from previous work on $CmBa_2Cu_3O_7$, which has a measured magnetic moment of $8.9(2)\mu_B$,[35] and $PrBa_2Cu_3O_7$,[36] in which the Cu moments

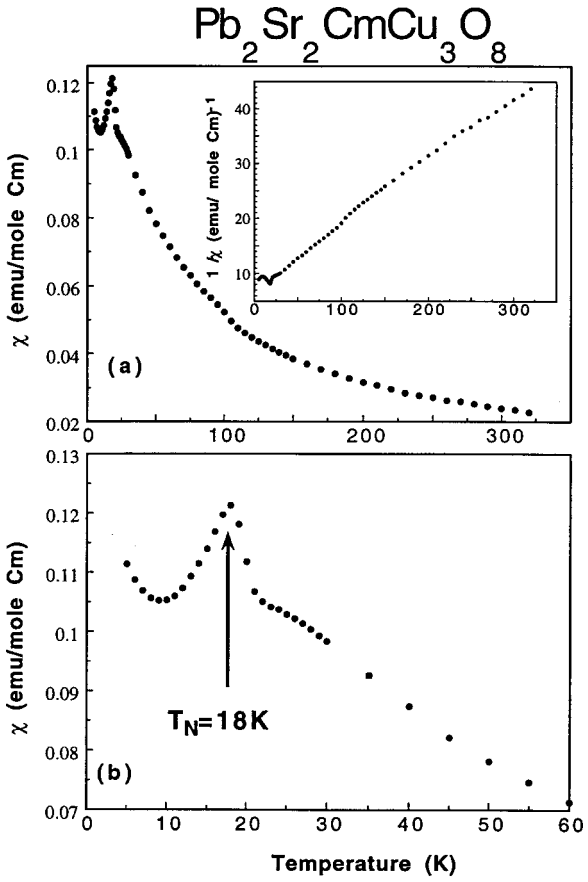

FIG. 5. (a) The temperature dependence of the magnetic susceptibility of $Pb_2Sr_2CmCu_3O_8$ and the inverse susceptibility is shown in the inset. (b) Magnetic susceptibility at low temperatures. The cusp at 18 K indicates the antiferromagnetic ordering of Cm ions in this compound.

order slightly above room temperature. In contrast to the observations from $Pb_2Sr_2CmCu_3O_8$ and $CmBa_2Cu_3O_7$, the measured susceptibility of Cm_2CuO_4 is $7.89(5)\mu_B$, which is consistent with local moments only on Cm^{3+}.[13]

An expanded view of low-temperature magnetic susceptibility data, shown in Fig. 5(b), reveals a cusp in the data centered at about 18 K. Similar cusps, attributed to the antiferromagnetic ordering of Cm moments, have been observed in Cm_2CuO_4 and $CmBa_2Cu_3O_7$ at 25 and 22 K, respectively.[35,37] Magnetic neutron diffraction experiments[13] unambiguously confirmed the origin of the transition at 25 K in Cm_2CuO_4 as the antiferromagnetic ordering of Cm spins. Although the small sample sizes used here prevented us from obtaining the magnetic ordering details from neutron diffraction, we conclude that the Cm spins antiferromagnetically order in $Pb_2Sr_2CmCu_3O_8$ at 18 K. This conclusion is based on the similarities in the temperature dependence of the magnetic susceptibility in these two compounds. The temperature dependence of the magnetic susceptibility in $Pb_2Sr_2Cm_{0.5}Ca_{0.5}Cu_3O_8$ did not show a cusp, therefore there is no indication for magnetic ordering of Cm ions in $x=0.5$ above 5 K. This result is consistent with the dilution of the magnetic ions by Ca in this compound.[38] Although the ordering is suppressed in the Ca compound, the strong mag-

netic interactions and hybridization with Cu-O planes that resulted in the magnetic ordering of the Cm moments in the parent phase will still be present in the Ca-doped samples.

Low-field magnetization data obtained from $Pb_2Sr_2Cm_{0.5}Ca_{0.5}Cu_3O_8$ showed no indication of a superconducting transition, although the sample was prepared under conditions that, for lanthanide-doped $Pb_2Sr_2R_{0.5}Ca_{0.5}Cu_3O_8$, result in bulk superconductivity. Whereas a slight variation in the Ca concentration (x) from 50% cannot be ruled out, our overall conclusion remains the same because superconductivity has been observed in other R analogs for wide range of $x(0.2<x<0.8)$.

IV. DISCUSSION

Single-phase samples of $Pb_2Sr_2CmCu_3O_8$ and $Pb_2Sr_2Cm_{1-x}Ca_xCu_3O_8$ have been prepared following synthetic procedures as optimized for $Pb_2Sr_2Pr_{1-x}Ca_xCu_3O_8$.[39] A combination of x-ray powder diffraction and Cm L_3-edge EXAFS data have been used to probe the atomic structures of these materials. The Cm analog of $Pb_2Sr_2RCu_3O_8$ is isostructural with the other R members of this series. The diffraction lines are indexed, and the positional parameters are refined in the Cmmm space group. As previously observed for the R denoting Y, Pr, and Tb analogs, the (1, 1, 4) and (2, 0, 5) peaks in the R for Cm sample are also much broader than (0, 0, 2), (0, 2, 0) and (0, 2, 5) peaks,[2,29–31] indicating the slight monoclinic distortion found for the lanthanide compounds is also present in the Cm sample.

The structural data, including the trends established in unit-cell lengths, cell volumes, and R-O bond distances, are all consistent with trivalent Cm in these samples. This result is confirmed by XANES spectroscopy and magnetic susceptibility data, which clearly show the presence of only Cm^{3+} in both the parent compound and the Ca-doped sample. This result is consistent with the overall redox chemistry of the rare earths and actinides in the known Cu-O superconductors.[2,4,8,13,39] Am and Ce are the most easily oxidized, from trivalent to tetravalent, of the f ions found in these systems.[3] Pr, Tb, and Cm can form selected tetravalent oxides, but have been found to be trivalent when associated with a Cu-O framework. Recently, it has been predicted that Am will be trivalent in Am_2CuO_4 and that superconductivity will be induced by Ce^{4+} doping for Am^{3+}.[40] This prediction is in contrast to the trend established to date by the redox-active f ions in these oxide systems.

Although $Pb_2Sr_2Cm_{1-x}Ca_xCu_3O_8$ is isostructural with all the superconducting $Pb_2Sr_2R_{1-x}Ca_xCu_3O_8$ compounds, and Cm is trivalent, there is no indication for superconductivity at temperatures down to 5 K. Whereas the Ce and Am analogs are also not superconducting, the f ions in both these cases are tetravalent. Both $Pb_2Sr_2Pr_{0.5}Ca_{0.5}Cu_3O_8$ and $Pb_2Sr_2Tb_{0.5}Ca_{0.5}Cu_3O_8$ are superconducting, although the Pr analog of the $RBa_2Cu_3O_7$ series is not, and the Tb analog does not form as a single-phase sample.

It was observed in an early work on $[La_{1-x}(Ba, Sr, Ca)_x]_2CuO_{2-\delta}$ that there is a strong correlation between superconductivity and the Cu-O bond lengths in the superconducting planes.[41] Considerably shorter Cu-O bonds were observed for superconducting samples, uncorrelated with the effective f-ion ionic radius. This effect was clearly demonstrated by the dependence of the superconducting transition temperature (T_c) on the lattice parameter a, which is an indirect measure of the planar O-Cu-O bondlength. The highest T_c was observed for the shortest a, and T_c was found to decrease with increasing a. As with other series, the Cu-O bond length is not exactly proportional to a in $Pb_2Sr_2R_{1-x}Ca_xCu_3O_8$, however, it can be assumed for comparison purposes that lattice parameters a and b are proportional to the lengths of O-Cu-O bond. In $Pb_2Sr_2Cm_{1-x}Ca_xCu_3O_8$, the lattice parameters a and b shrink with increasing Ca concentrations, similar to the observed behavior in the other R analogs.[2,20] The relative change in Cm is similar to other R except Pr, where relatively larger contractions in a and b are observed with Ca doping. The a and b axes in 50% Ca-doped Pr compounds are found to be significantly smaller than those of the Cm analog, despite the fact that the ionic radius of Pr is slightly larger than that of Cm. Since $Pb_2Sr_2Cm_{0.5}Ca_{0.5}Cu_3O_8$ is not superconducting and it has the largest a and b, it is also consistent with the trend noticed by Kishio *et al.*[41] that compounds with the largest Cu-O bond lengths have the lowest T_cs. A careful comparison of the reported lattice parameters in the $RBa_2Cu_3O_7$ series[35] also supports this trend. Although the ionic radius of Cm is smaller than that of Nd, a and b in $CmBa_2Cu_3O_7$, which is not a superconductor, are greater than those of other superconducting R.

TABLE III. Magnetic ordering temperatures (T_N) of R in three superconducting systems. T_N of Cm is higher than all other R, indicating that the magnetic interactions are very strong in Cm compounds (Refs. 1, 9, 10, 13, 31, 35, 42–44, 47–52).

R	$RBa_2Cu_3O_7$	R_2CuO_4	$Pb_2Sr_2RCu_3O_8$
Pr	17.0	No ordering	6.0
Nd	1.5	1.6	1.7
Sm	0.6	5.95	1.1
Gd	2.2	6.4	2.3
Tb	Does not form	9	5.3
Dy	1.3	7	0.9
Cm	22.0	25.0	18.0

The antiferromagnetic ordering temperatures (T_N) of Cm in three different high-T_c related compounds along with some of their rare-earth analogs are given in Table III. The Cm magnetic ordering temperature of 18 K in $Pb_2Sr_2CmCu_3O_8$ is the largest in the series. In $Pb_2Sr_2GdCu_3O_8$, the Gd spins order antiferromagnetically at 2.3 K.[42] Although Gd and Cm both have an f^7 configuration, and both have a spherically symmetric ground state with a large magnetic moment, there is a significant difference in their ordering temperatures. In the R_2CuO_4 series, similarities are observed in the magnetic properties of Gd and Cm, which have ordering temperatures of 6.4 and 25 K, respectively.[13,43] Both have the same magnetic structure and three-dimensional (3D) behavior, and the nearest-neighbor distances are almost equal in all three directions. Since the maximum temperature expected for dipole-type magnetic in-

teractions is about 2 K, it has been concluded that exchange interactions play an important role for the magnetic ordering in the R_2CuO_4 series.[44] Although 3D magnetic ordering of the f moments is observed in the $RBa_2Cu_3O_7$ and $Pb_2Sr_2RCu_3O_8$ series, the ordering shows a 2D-like magnetic behavior, which is observed even above T_N.[31,44] This behavior originates naturally from the 2D-like crystal structure. The *R-R* nearest-neighbor distance along the *c* axis (~15.8 Å) in $Pb_2Sr_2RCu_3O_8$ is about four times larger than that in the *a-b* plane (~3.9 Å). Therefore *R* magnetic coupling within the *a-b* plane is expected to be much stronger than the coupling between planes, resulting in the observed 2D behavior. The Gd spins in $Pb_2Sr_2GdCu_3O_8$ order at 2.3 K and dipole rather than exchange magnetic interactions are responsible for the magnetic ordering. In contrast, Cm in $Pb_2Sr_2CmCu_3O_8$ orders at 18 K, where it is clear that Cm-Cm exchange interactions play the pivot role. That the exchange interactions are clearly more dominant in the magnetic behavior of the Cm-based materials than in any of the lanthanide analogs is consistent with the known characteristics of the Cm $5f$ orbitals, which have a larger radial extent than their $5f$ counterparts and therefore are more delocalized.[4] Cm states may more easily hybridize with the CuO bands and make the exchange interactions very strong in the *a-b* plane as well as along the *c* direction. The nature of the magnetic interactions is different in Cm and Gd in $Pb_2Sr_2RCu_3O_8$, therefore the magnetic structure may be also different in these compounds.

The Cm analogs of all the Cu-O series studied to date have the highest T_Ns within their series (Table III). This result indicates that the Cm magnetic exchange interactions are very strong. Interestingly, all compounds with anomalously high T_N (Cm compounds and $PrBa_2Cu_3O_7$) are not superconducting; an observation that points toward the strong connection between magnetism and superconductivity. Our measurements on $Pb_2Sr_2Cm_{1-x}Ca_xCu_3O_8$ confirm the hybridization effects on superconductivity. In Pr compounds, superconductivity appears to be dependent on the splitting of the $^3H_4$ Russell-Saunders ground level.[8,39] The superconducting critical temperature appears to correlate with the moment of the Pr ground state. Cm, with its spherically symmetric $^8S_{7/2}$ ground state, is uninfluenced to first order by the crystal field, and therefore Cm always carries a large moment. All Cm high-T_c related compounds have been found to be nonsuperconducting. Cm^{3+} $5f$ orbitals are not as well localized as their $4f$ counterparts, and can easily hybridize with the CuO planar states responsible for superconductivity and situated near the Cm ion. The large magnetic moment on Cm can affect the superconductivity by breaking the Cooper pairs. The strong bonding between the Cm magnetic *f* states and the CuO band will make the indirect magnetic exchange interactions very strong and induce the Cm spins to magnetically order at unusually high temperatures. Strong Cm-Cm magnetic exchange interactions, implied by the high magnetic ordering temperature, are expected to be mediated along the *c* direction through the Cu-O layers implying a relatively strong Cm-Cu coupling. Such a coupling has been previously reported in $PrBa_2Cu_3O_7$.[45,46] These Cm-Cu interactions influence the Cu sublattice magnetic properties sufficiently to suppress superconductivity in the Ca-doped compound. A full understanding of this correlation between superconductivity and T_c suppression requires further investigation.

ACKNOWLEDGMENTS

This work benefited from the use of the Advanced Photon Source, and the infrastructures provided by the Actinide Facility and the BESSRC CAT, all at Argonne National Laboratory. This work was supported by the DOE-Basic Energy Sciences, Chemical Sciences and Material Sciences (APS) under Contract No. W-31-109-ENG-38.

[1] U. Staub and L. Soderholm, in *Handbook on the Physics and Chemistry of Rare Earths*, edited by J. K. A. Gschneidner, L. Eyring, and M. B. Maple (Elsevier Science, New York, 2000), Vol. 30, pp. 491–545.

[2] S. Skanthakumar and L. Soderholm, Phys. Rev. B **53**, 920 (1996).

[3] L. Soderholm, C. Williams, S. Skanthakumar, M. R. Antonio, and S. Conradson, Z. Phys. B: Condens. Matter **101**, 539 (1996).

[4] L. Soderholm and U. Staub, in *Electron Correlations and Magnetic Properties*, edited by A. Gonis, N. Kioussis, and M. Ciftan (Kluwer Academic, New York, 1999), pp. 115–136.

[5] L. F. Schneemeyer, R. J. Cava, A. C. W. P. James, P. Marsh, T. Siegrist, J. V. Waszczak, J. J. Krajewski, W. P. Peck, Jr., R. L. Opila, S. H. Glarum, J. H. Marshall, R. Hull, and J. M. Bonar, Chem. Mater. **1**, 548 (1989).

[6] R. J. Cava, B. Batlog, J. J. Krajewski, L. W. Rupp, L. F. Schneemeyer, T. Siegrist, R. B. van Dover, P. Marsh, W. F. Peck, P. K. Gallagher, S. H. Glarum, J. H. Marshall, R. C. Farrow, J. V. Waszczak, R. Hull, and P. Trevor, Nature (London) **336**, 211 (1988).

[7] J. S. Xue, M. Reedyk, J. E. Greedan, and T. Timusk, J. Solid State Chem. **102**, 492 (1993).

[8] U. Staub, S. Skanthakumar, L. Soderholm, and R. Osborn, J. Alloys Compd. **250**, 581 (1997).

[9] W. T. Hsieh, W.-H. Li, K. C. Lee, J. W. Lynn, J. H. Shieh, and H. C. Ku, J. Appl. Phys. **76**, 7124 (1994).

[10] J. H. Shieh, H. C. Ku, and J. C. Ho, Phys. Rev. B **50**, 3288 (1994).

[11] J. Röhler, in *Handbook on the Physics and Chemistry of Rare Earths*, edited by J. K. A. Gschneidner, L. Eyring, and S. Hüfner (North-Holland, Amsterdam, 1987), Vol. 10, p. 453.

[12] A. C. Larson and R. B. V. Dreele, Los Alamos National Laboratory, Los Alamos, Report No. NM 87545, 1990 (unpublished).

[13] L. Soderholm, S. Skanthakumar, and C. W. Williams, Phys. Rev. B **60**, 4302 (1999).

[14] F. W. Lytle, in *Applications of Synchrotron Radiation*, edited by H. Winick, D. Xian, M. H. Ye, and T. Huang (Gordon and Breach, New York, 1989), Vol. 4, p. 135.

[15] T. Ressler, J. Synchrotron Radiat. **5**, 118 (1998).

[16] J. J. Rehr, J. M. d. Leon, S. I. Zabinsky, and R. C. Albers, J. Am. Chem. Soc. **113**, 5135 (1991).
[17] L. Soderholm, M. R. Antonio, C. W. Williams, and S. R. Wasserman, Anal. Chem. **71**, 4622 (1999).
[18] S. D. Conradson, I. A. Mahamid, D. L. Clark, N. J. Hess, E. A. Hudson, M. P. Neu, P. D. Palmer, W. H. Runde, and C. D. Tait, Polyhedron **19**, 599 (1998).
[19] S. Bertram, G. Kaindl, J. Jove, M. Pages, and J. Gal, Phys. Rev. Lett. **63**, 2680 (1989).
[20] J.-E. Jorgensen and N. H. Anderson, Physica C **235–240**, 877 (1994).
[21] R. D. Shannon, Acta Crystallogr., Sect. A: Cryst. Phys., Diffr., Theor. Gen. Crystallogr. **A32**, 751 (1976).
[22] M. A. Subramanian, J. Gopalakrishnan, C. C. Torardi, P. L. Gai, E. D. Boyes, T. R. Askew, R. B. Flippen, W. E. Farneth, and A. W. Sleight, Physica C **157**, 124 (1989).
[23] C. Chaillout, O. Chmaissen, J. J. Capponi, T. Fournier, G. McIntyre, and M. Marezio, Physica C **175**, 293 (1991).
[24] R. J. Cava, M. Marezio, J. J. Krajewski, W. F. Peck, Jr., A. Santoro, and F. Beech, Physica C **157**, 272 (1989).
[25] M. Marezio, A. Santoro, J. J. Capponi, E. A. Hewat, R. J. Cava, and F. Beech, Physica C **169**, 401 (1990).
[26] J.-E. Jørgensen and N. H. Andersen, Acta Chem. Scand. **45**, 19 (1991).
[27] J. S. Xue, J. E. Greedan, and M. Maric, J. Solid State Chem. **102**, 501 (1993).
[28] H. Fujishita, M. Sato, Y. Morii, and S. Funahashi, Physica C **210**, 529 (1993).
[29] J.-E. Jorgensen, Solid State Commun. **80**, 613 (1991).
[30] U. Staub, L. Soderholm, S. Skanthakumar, P. Pattison, and K. Conder, Phys. Rev. B **57**, 5535 (1998).
[31] S. Skanthakumar, L. Soderholm, and R. Movshovich, J. Alloys Compd. **303-304**, 298 (2000).
[32] S. Skanthakumar and L. Soderholm (unpublished).
[33] J.-E. Jorgensen and N. H. Anderson, Acta Chem. Scand. **46**, 122 (1992).
[34] J.-E. Jorgensen and N. H. Anderson, Physica C **218**, 43 (1994).
[35] L. Soderholm, G. L. Goodman, U. Welp, C. W. Williams, and J. Bolender, Physica C **161**, 252 (1989).
[36] S. Skanthakumar, J. W. Lynn, N. Rosav, G. Cao, and J. E. Crow, Phys. Rev. B **55**, R3406 (1997).
[37] L. Soderholm, C. W. Williams, and U. Welp, Physica C **179**, 440 (1991).
[38] T. Oguchi and T. Obokata, J. Phys. Soc. Jpn. **27**, 1111 (1969).
[39] U. Staub, L. Soderholm, S. Skanthakumar, R. Osborn, and F. Fauth, Europhys. Lett. **39**, 663 (1997).
[40] H. A. Blackstead and J. Dow, Phys. Rev. B **59**, 14 593 (1999).
[41] K. Kishio, K. Kitazawa, N. Sugii, S. Kanbe, K. Fueki, H. Takagi, and S. Tanaka, Chem. Lett. **1987**, 635.
[42] C. C. Lai, J. H. Shieh, B. S. Chiou, J. C. Ho, and H. C. Ku, Phys. Rev. B **49**, 1499 (1994).
[43] T. Chattopadhyay, P. J. Brown, A. A. Stepanov, P. Wyder, J. Voiron, A. I. Zvyagin, S. N. Barilo, D. I. Zhigunov, and I. Zobkalo, Phys. Rev. B **44**, 9486 (1991).
[44] J. W. Lynn and S. Skanthakumar, in *Handbook on the Physics and Chemistry of Rare Earths*, edited by J. K. A. Gschneidner, L. Eyring, and M. B. Maple (Elsevier Science, New York, in press).
[45] S. Uma, W. Schnelle, E. Gmelin, G. Rangarajan, S. Skanthakumar, J. W. Lynn, R. Walter, T. Lorenz, B. Buchner, E. Walker, and A. Erb, J. Phys.: Condens. Matter **10**, L33 (1998).
[46] S. Skanthakumar, J. W. Lynn, N. Rosov, G. Cao, and J. E. Crow, Phys. Rev. B **55**, R3406 (1997).
[47] S. Obradors, P. Visani, M. A. d. l. Torre, M. B. Maple, M. B. Tovar, F. Perez, P. Bordet, J. Chenavas, and D. Chateigner, Physica C **213**, 81 (1993).
[48] H. Okada, M. Takano, and Y. Takeda, Phys. Rev. B **42**, 6813 (1990).
[49] I. W. Sumarlin, S. Skanthakumar, J. W. Lynn, J. L. Peng, Z. Y. Li, W. Jiang, and R. L. Greene, Phys. Rev. Lett. **68**, 2228 (1992).
[50] C. R. Shih, T. H. Meen, Y. C. Chen, and H. D. Yang, Phys. Rev. B **50**, 9619 (1994).
[51] S. Y. Wu, W. T. Hsieh, W.-H. Li, K. C. Lee, J. W. Lynn, and H. D. Yang, J. Appl. Phys. **75**, 6598 (1994).
[52] U. Staub, L. Soderholm, S. Skanthakumar, S. Rosenkranz, C. Ritter, and W. Kagunya, Z. Phys. B: Condens. Matter **104**, 37 (1997).